The Journal of Experimental Biology 216, 3873-3885

doi:10.1242/jeb.087890

RESEARCH ARTICLE

Differential expression and novel permeability properties of three aquaporin 8 paralogs from seawater-challenged Atlantic salmon smolts

Morten B. Engelund[1,*], François Chauvigné[2], Birgitte Mønster Christensen[3], Roderick Nigel Finn[4,5], Joan Cerdà[2] and Steffen S. Madsen[1]

[1]Institute of Biology, University of Southern Denmark, Campusvej 55, 5230 Odense, Denmark, [2]Institut de Recerca i Tecnologia Agroalimentàries (IRTA) – Institut de Ciències del Mar, Consejo Superior de Investigaciones Científicas (CSIC), Passeig Marítim de la Barceloneta, 37-49, 08003 Barcelona, Spain, [3]Department of Biomedicine, Anatomy, Wilhelm Meyers Álle 3, Aarhus University, 8000 Aarhus, Denmark, [4]Department of Biology, Bergen High Technology Centre, University of Bergen, 5020 Bergen, Norway and [5]Institute of Marine Research, Nordnes, 5817 Bergen, Norway

*Author for correspondence (mengelund@biology.sdu.dk)

SUMMARY

Aquaporins may facilitate transepithelial water absorption in the intestine of seawater (SW)-acclimated fish. Here we have characterized three full-length *aqp8* paralogs from Atlantic salmon (*Salmo salar*). Bayesian inference revealed that each paralog is a representative of the three major classes of *aqp8aa*, *aqp8ab* and *aqp8b* genes found in other teleosts. The permeability properties were studied by heterologous expression in *Xenopus laevis* oocytes, and the expression levels examined by qPCR, immunofluorescence and immunoelectron microscopy, and immunoblotting of membrane fractions from intestines of SW-challenged smolts. All three Aqp8 paralogs were permeable to water and urea, whereas Aqp8ab and -8b were, surprisingly, also permeable to glycerol. The mRNA tissue distribution of each paralog was distinct, although some tissues such as the intestine showed redundant expression of more than one paralog. Immunofluorescence microscopy localized Aqp8aa(1+2) to intracellular compartments of the liver and intestine, and Aqp8ab and Aqp8b to apical plasma membrane domains of the intestinal epithelium, with Aqp8b also in goblet cells. In a control experiment with rainbow trout, immunoelectron microscopy confirmed abundant labeling of Aqp8ab and -8b at apical plasma membranes of enterocytes in the middle intestine and also in subapical vesicular structures. During SW challenge, Aqp8ab showed significantly increased levels of protein expression in plasma-membrane-enriched fractions of the intestine. These data indicate that the Atlantic salmon Aqp8 paralogs have neofunctionalized on a transcriptional as well as a functional level, and that Aqp8ab may play a central role in the intestinal transcellular uptake of water during SW acclimation.

Supplementary material available online at http://jeb.biologists.org/cgi/content/full/216/20/3873/DC1

Key words: aquaporin, evolution, osmoregulation, salmon, intestine, neofunctionalization.

Received 7 March 2013; Accepted 2 July 2013

INTRODUCTION

The Atlantic salmon (*Salmo salar* Linnaeus 1758) is a euryhaline teleost with an anadromous life cycle during which it periodically inhabits freshwater (FW) as well as seawater (SW) environments. The internal osmolarity is maintained at approximately one-third of full-strength SW irrespective of the environment, and thus there are strong hyperosmotic gradients with respect to FW (~1 mOsm) and hyposmotic gradients with respect to SW (~1000 mOsm) (Evans et al., 2005). In FW, ions are lost to the environment by diffusion and are replaced by active absorption in the gills (Evans et al., 2005; Hwang et al., 2011) and through extraction of solutes from food particles in the intestine (Buddington and Diamond, 1987; Sundell et al., 2003). Excess water is excreted by the kidney and valuable solutes and ions are reabsorbed by the proximal and distal segments of the nephron (Beyenbach, 2004; McDonald, 2007). In SW, fluxes of ions and water are reversed. To compensate for such water loss, salmon begin drinking shortly after transfer to SW (Smith, 1932; Usher et al., 1988) and the ingested water is absorbed passively in concert with ions during passage through the gastrointestinal tract (Ando et al., 2003; Sundell and Sundh, 2012; Wood and Grosell, 2012). Excess ions are actively excreted over the gill, predominantly through transcellular and paracellular routes in association with ionocytes in the gill filaments (Karnaky, 1986; Hiroi et al., 2005; Tipsmark et al., 2008). Divalent ions are excreted by the kidney and intestine and an overall decrease in glomerular filtration rate occurs in order to conserve water (Brown et al., 1978; Brown et al., 1980). Important water fluxes also occur in other tissues such as the liver and gall bladder during the formation of bile (Grosell et al., 2000) or in marine teleost oocytes undergoing meiotic maturation (e.g. Fabra et al., 2005; Fabra et al., 2006; Zapater et al., 2011).

Recent studies have highlighted an important physiological role of transmembrane water channels (aquaporins) that transport water and small, noncharged solutes such as urea and glycerol for the maintenance of fluid homeostasis in fishes exposed to FW or SW environments (reviewed by Cerdà and Finn, 2010; Sundell and Sundh, 2012). Compared with mammals, however, teleosts have been shown to encode duplicate copies of most aquaporin orthologs, but up to three copies of the *aqp8* gene, consistent with both tandem

and genomic duplication events early in the evolution of this lineage (Cerdà and Finn, 2010; Tingaud-Sequeira et al., 2010; Finn and Cerdà, 2011). Within some families of teleosts, such as Salmonidae, yet another genome duplication is known to have occurred (Davidson et al., 2010; Moghadam et al., 2011), making it a cumbersome task to characterize all existing paralogs even for one species.

To date, the piscine aquaporin superfamily has only been characterized in the diploid zebrafish (*Danio rerio*) (Tingaud-Sequeira et al., 2010), while other species of teleost have been examined with respect to basal expression patterns of selected aquaporins within osmoregulatory tissues (Cutler and Cramb, 2002; Lignot et al., 2002; Martinez et al., 2005a; Martinez et al., 2005b; Raldúa et al., 2008; Tingaud-Sequeira et al., 2010; Tipsmark et al., 2010; Madsen et al., 2011). Although there is some consensus on the expression pattern of each paralog, there is emerging evidence that even closely related aquaporins, such as the tandemly duplicated *aqp1aa* and *aqp1ab* genes and alternatively duplicated *aqp8* paralogs, have neofunctionalized in relation to their regulation and function (Martinez et al., 2005a; Martinez et al., 2005b; Tipsmark et al., 2010; Madsen et al., 2011; Finn and Cerdà, 2011; Zapater et al., 2011). In the stenohaline FW zebrafish, *aqp8* is present as three paralogs (*aqp8aa*, *-8ab* and *-8b*) and fragments of each have been found in a partial transcriptome (EST library) of the Atlantic salmon (Tingaud-Sequeira et al., 2010; Cerdà and Finn, 2010; Engelund and Madsen, 2011). In mammals, such as rats, only one AQP8 is expressed, and it is found in the proximal kidney tubules, hepatocytes, testes, salivary gland and intestine (Elkjær et al., 2001). In teleosts such as the European eel (*Anguilla anguilla*), Japanese eel (*Anguilla japonica*), zebrafish and Atlantic salmon, several *aqp8* transcripts have been located in some of the same tissues, although each paralog showed a distinct tissue mRNA expression pattern (Cutler et al., 2009; Kim et al., 2010; Tingaud-Sequeira et al., 2010; Tipsmark et al., 2010). Because of the extra round of genome duplication in salmonids, more *aqp8*s may exist in this species than in zebrafish and the present study probably does not reveal the full complement of *aqp8*s in Atlantic salmon. Specifically, an extra *aqp8aa* was uncovered based on preliminary data from the Atlantic salmon genome during this study. These two paralogs, *aqp8aa1* and *aqp8aa2*, are 92% identical on a nucleotide level and share 91% identical amino acid residues. Once the genome is published, more paralogs might be uncovered, contributing to the evidence of the extra round of genome duplication in salmonids. However, the focus of this study is representatives of the three main types of *aqp8*, which are known from the comprehensive studies on zebrafish (Tingaud-Sequeira et al., 2010; Cerdà and Finn, 2010) in order to uncover whether neofunctionalization of these paralogs is important for regulation of water balance.

During SW acclimation, Atlantic salmon *aqp8ab* mRNA is strongly upregulated in intestinal segments, indicating a possible role for this paralog in water balance (Tipsmark et al., 2010). Similar results were found for European and Japanese eels, where SW-acclimated animals showed higher levels of *aqp8* mRNA in the intestine (Cutler et al., 2009; Kim et al., 2010). The involvement of Aqp8 in the SW acclimation of Atlantic salmon was further supported by recent work in our laboratory, where a homologous antibody detected Aqp8ab in the brush borders and lateral membranes of enterocytes (Madsen et al., 2011).

In the present study, we set out to expand the knowledge of Aqp8 biology in Atlantic salmon by investigating the tissue distribution of *aqp8* mRNAs and determine the cellular locations of Aqp8aa(1+2), -8ab and -8b proteins using homologous antibodies. We additionally examined the protein expression of Aqp8ab and Aqp8b in two intestinal segments to establish whether the suggested role of Aqp8ab during SW acclimation (Tipsmark et al., 2010) could be confirmed at the protein level and whether differences existed between the paralogs. The permeability properties of the three paralogs were investigated in *Xenopus laevis* oocytes in order to reveal potential neofunctionalization, which could shed light on whether tissue-specific expression patterns are linked to functional diversity.

MATERIALS AND METHODS

Animals

Atlantic salmon presmolts were obtained from the Danish Centre for Wild Salmon (Randers, Denmark). The fish spent the spring in outdoor tanks under natural light and temperature conditions and were moved to the university campus in June 2010 to an indoor aquarium with biofiltered recirculated FW where a photoperiod of 12 h:12 h light:dark and a constant temperature of 14°C was upheld. In September 2010, a group of fish was moved to a tank containing artificial 25 ppt SW (Red Sea salt, Eliat, Israel), where they remained for at least 3 weeks prior to sampling. The fish were fed *ad libitum* using commercial fish pellets and food was generally withheld 3 days before an experiment. Fish were anesthetized with 0.2 ppt phenoxy ethanol and euthanized by cutting the spinal cord and pithing the brain before samples for RNA analysis and histology were taken. Long-term SW- or FW-acclimated salmon were then used for the tissue screening of *aqp8* transcripts while intestine and liver from SW-acclimated salmon were used for immunofluorescence microscopy. Middle intestine from long-term SW-acclimated rainbow trout (*Oncorhynchus mykiss*; ~40 g) obtained from Lihme Dambrug (Randbøl, Denmark) was used for immunoelectron microscopy. All experimental procedures were approved by the Danish Animal Experiments Inspectorate in accordance with the European Convention for the Protection of Vertebrate Animals used for Experiments and Other Scientific Purposes (86/609/EØF).

SW acclimation experiment

In late April 2012, 1-year-old smolts (20–30 g, N=100) were transferred to a tank containing 25 ppt SW at the Danish Centre for Wild Salmon and 10 fish were anesthetized and sampled as described above following 6, 24, 72 and 168 h in SW. At the same time, a control group of smolts (N=100) was sham-transferred to a tank containing FW and sampled accordingly. Ten smolts were sampled prior to sham or SW transfer to represent time point 0 h.

Cloning of Atlantic salmon aquaporins *aqp8aa1*, *aqp8ab* and *aqp8b*

Full-length sequences of Atlantic salmon *aqp8* mRNAs were cloned using RNA from the middle intestine for *aqp8ab* and *aqp8b* and from the liver for *aqp8aa1*. RNA was purified using TRIsure (DNA Technology, Risskov, Denmark) according to the manufacturer's instructions. cDNA synthesis was performed with an oligo$(dT)_{15}$ primer using the DyNAmo cDNA Synthesis Kit (Thermo Scientific, Søborg, Denmark) according to the manufacturer's instructions. The full mRNA sequence for *aqp8ab* and *aqp8b* was readily available from the EST database for Atlantic salmon at www.ncbi.nlm.nih.gov based on previous annotations (see Table 1) (Cerdà and Finn, 2010; Tipsmark et al., 2010). The full *aqp8ab* cDNA was amplified in one PCR reaction using the cloning primers listed in Table 1. PCR conditions were an initial denaturing for 3 min at 94°C followed by 35 cycles of 94°C for 45 s, 59°C for 45 s and 72°C for 1 min ending with a final elongation at 72°C for 12 min. Cloning primers included restriction enzyme sequences for *Bgl*II and *Eco*RV in the 5′ and 3′

Table 1. Primers used for cloning and qPCR of Atlantic salmon aquaporin 8 paralogs

Primer	Primer sequence 5′→3′	Amplicon size (bp)
8aa1OFP	GTAAGTGACACAGAGAGCAGCAGTA	859
8aa1ORP	ATGCCCTATGTCTCCAAGATAAC	
8aa1CFP	ACT*AGATCT***ATG**TCTGTGATAGAGTCAAAGAC	816
8aa1CRP	AGC*GATATC***TTA**CTTCAGAACAAGACGTGTCT	
8abCFP	ACT*AGATCT***ATG**GGAGTTGAGAAAATGGAGCT	798
8abCRP	CGC*GATATC***TCA**CTTCATGATGATTCGTGTCTT	
8bbOFP	TCTCTCCAAACTCCTTTCCA	858
8bbORP	TGGCACTGCATGTAACAACA	
8bbCFP	ACT*AGATCT***ATG**ACAGAAGGGACAATGGAAC	798
8bbCRP	CGC*GATATC***TTA**CTTCATGAGAATACGTGTCTT	
8aa(1+2)QPCRFP*	TCATGACCCTCTTCCTGTCC	145
8aa(1+2)QPCRRP*	GGGTTCATACACCCTCCAGA	
8abQPCRFP*	GGAGCTGCCATGTCAAAGAT	159
8abQPCRRP*	CGCCCCTAGCAATACTACCA	
8bQPCRFP2 3UTR	GACACGCCTGCTCATTCG	71
8bQPCRRP2 3UTR	GTCTCCACCACCATTCAACAA	

Primers for aquaporin paralogs were constructed using the following ESTs: *aqp8aa(1+2)*: CU071487 and DW573347; *aqp8ab*: Ssa.15811 (formerly annotated as AQP-8b); *aqp8b*: ACN11279.

*Primers previously published (Tipsmark et al., 2010).

Bold marks start and stop codons. *Italic* marks BglII and EcoRV restriction sites. O(F/R)P: Primers annealing outside coding sequence, used for nested PCR. C(F/R)P: Primers used for cloning of the full cDNA sequence.

ends, respectively. The *aqp8b* cDNA was obtained using a nested PCR design. First, 35 cycles of PCR as explained above were performed with primers aligning outside the coding sequence (Table 1). This was followed by 15 cycles of PCR using cloning primers (Table 1) with a slight increase in annealing temperature of the PCR reaction to 61°C. The *aqp8aa1* cDNA was obtained by PCR using primers aligning to the 3′UTR of rainbow trout *aqp8aa* and the 5′UTR of the Atlantic salmon *aqp8aa1*. After the initial PCR reaction using these primers, another PCR reaction was performed for 35 cycles using cloning primers (Table 1). Annealing temperature was 61°C and the other parameters of the PCR reaction were the same as described above. The transcripts were ligated into the pT7Ts oocyte expression vector, which was then used as a template for *in vitro* transcription (see below). Each paralog was sequenced in both directions to ensure a complete cDNA.

Phylogenetic analysis

Deduced amino acid sequences of the isolated Atlantic salmon mRNAs were aligned with other teleost Aqp8 orthologs retrieved from public databases (Ensembl v70 and GenBank) using the MAFFT (v7.017b) and T-Coffee (9.03.r1318) software packages (Notredame et al., 2000; Katoh and Toh, 2008). Amino acid alignments were converted to codon alignments using Pal2Nal (Suyama et al., 2006) and molecular phylogenies inferred using Bayesian [M_r Bayes v3.2.0; 5 million generations (Ronquist and Huelsenbeck, 2003)] and maximum likelihood [PAUP v4b10-x86-macosx (Swafford, 2002)] protocols as described previously (Zapater et al., 2011; Zapater et al., 2013).

Water permeability of *X. laevis* oocyte expressing salmon aquaporin 8

Atlantic salmon *aqp8* cDNAs were cloned into the *Eco*RV/*Bgl*II sites of the oocyte expression vector pT7Ts (Deen et al., 1994). The cRNAs were synthesized as described previously (Deen et al., 1994) and microinjected into *X. laevis* stage V–VI oocytes. Oocytes were maintained in 200 mOsm modified Barts solution (MBS) [in mmol l^{-1}: 0.33 $Ca(NO_3)_2$, 0.4 $CaCl_2$, 88 NaCl, 1 KCl, 2.4 $NaHCO_3$, 0.82 $MgSO_4$, 10 4-(2-hydroxyethyl)-1-piperazine-ethanesulfonic acid (HEPES) pH 7.5] and injected with 50 nl of water containing 1–10 ng cRNA of one of the three salmon aquaporin 8 paralogs. Control oocytes were not injected as injection does not affect the water permeability of oocytes (data not shown). After 24 h, the oocytes were manually defolliculated and, following another 24 h, the water permeability of the oocytes was determined by measuring the time-course changes in the relative volume of the oocytes when incubated in 10-fold diluted MBS. The volume of the oocyte was determined by recording the maximal surface area of the oocyte every 2 s using time-lapse microscopy. Assuming that the oocyte is a perfect sphere, the relative volume change can then be calculated from the obtained surface area. The osmotic water permeability (P_f) was determined according to the following equation:

$$P_f = \frac{V_0\left[\frac{d(V/V_0)}{dt}\right]}{S \cdot V_w(\mathrm{Osm}_{in} - \mathrm{Osm}_{out})}, \quad (1)$$

where $d(V/V_0)/dt$ is the relative volume change of the oocyte with time incubated in the diluted medium, S is the surface area of the oocyte, V_w is the molar volume of water (18 cm^3) and Osm_{in} and Osm_{out} are the respective osmolalities of the solution inside and outside the oocyte. Inhibition of water transport by mercury was investigated by incubating oocytes in MBS containing 0.1 mmol l^{-1} $HgCl_2$ for 15 min prior to measurement. Recovery of water transport was measured by transferring $HgCl_2$-incubated oocytes through two washes with clean MBS to a solution of MBS with 5 mmol l^{-1} mercaptoethanol for 15 min prior to measurement.

Urea and glycerol uptake of *X. laevis* oocytes expressing salmon aqp8

Oocytes were injected with 50 nl of water or water containing 15 ng cRNA of a salmon *aqp8* paralog. Groups of 10 oocytes were incubated in 200 µl of MBS containing 20 µCi of [1,2,3-^{3}H]glycerol (50 Ci mmol l^{-1}) or [^{14}C]urea (58 mCi mmol l^{-1}) at room temperature. Cold solute was added to give a final concentration of 1 mmol l^{-1}. After 10 min, which included zero time for subtraction of the signal from externally bound solute, oocytes were washed rapidly in ice-cold MBS three times, and individual oocytes were then dissolved in 5% sodium dodecyl sulfate (SDS) for scintillation counting.

Tissue screening of salmon aquaporin 8 paralogs

Expression of salmon aquaporin mRNA in various tissues has previously been reported for *aqp8aa* and *aqp8ab* (Tipsmark et al., 2010) but was repeated in the present study for comparison with *aqp8b*. Total RNA was extracted from 14 different tissues of four Atlantic salmon as explained above. The RNA was subjected to DNase treatment with RQ1 RNase-Free DNase (Promega Biotech AB, Stockholm, Sweden) according to manufacturer's protocol. Synthesis of cDNA took place with the use of the High Capacity cDNA Reverse Transcription Kit (Applied Biosystems, Carlsbad, CA, USA). Real-time quantitative PCR (qPCR) was performed on an Mx3000p instrument (Stratagene, La Jolla, CA, USA) using the primers listed in Table 1. Primers for *aqp8aa* and *aqp8ab* were the same as reported in Tipsmark et al. (Tipsmark et al., 2010) and primers for *aqp8b* were designed using Primer 3 software (Rozen and Skaletsky, 2000). Preliminary data from the Atlantic salmon genome became available during the publication process of this study and showed that two *aqp8aa* paralogs (*aqp8aa1* and *aqp8aa2*) exist and the primers designed for qPCR are unable to distinguish between these two paralogs as they are 92% identical in the coding sequence. Results for this paralog are therefore named *aqp8aa(1+2)*. BlastN of each primer pair against the cloned sequence of each paralog showed no similarity other than against the paralog for which the primers were designed. For each paralog, the PCR product was validated by agarose gel electrophoresis and melting curve analysis. A two-step standard qPCR reaction (95°C for 30 s and 60°C for 1 min for 40 cycles) was performed using SYBR Green Jumpstart Taq Readymix (Sigma-Aldrich, St Louis, MO, USA). Total reaction volume was 25 µl and primers were used at a concentration of 150 nmol l^{-1}. The relative expression of the *aqp8* paralogs was normalized to the expression of elongation factor 1a (*ef1a*) according to Olsvik et al. (Olsvik et al., 2005). Efficiency of amplification (E_a) for each set of primers was calculated by standard curve analysis of increasing diluted solutions of cDNA according to Pfaffl (Pfaffl, 2001). Normalized expression of each paralog was then calculated as:

$$C_n = \left(1 + E_{a,\text{target}}\right)^{-C_{t,\text{target}}} / \left(1 + E_{a,\text{EF1a}}\right)^{-C_{t,\text{EF1a}}}, \quad (2)$$

where C_t is the threshold cycle and C_n is the relative copy number of the target gene.

Primary antibodies

The homologous polyclonal antibodies used in this study were raised in rabbits by BioGenes (Berlin, Germany). A synthetic peptide corresponding to a N-terminal epitope (Aqp8aa1: CFTVAGADTGDSGPG-amide; Aqp8ab: CGHSTLMSGTKKPTP-amide; Aqp8b: CMASDSKKAPVKPPN-amide) for each paralog was used to immunize the rabbits and the collected antisera were affinity purified against the antigenic peptide by BioGenes [Aqp8ab (Madsen et al., 2011)] or by use of the SulfoLink Immobilization Kit for Peptides (Aqpp8aa1 and Aqp8b; present study) (Thermo Scientific, Waltham, MA, USA) according to the manufacturer's instructions. For immunofluorescence and immunoelectron microscopy, serum was used. Cross-reactivity of each antibody toward the other paralogs was minimal, as shown by incubation of each antibody against a crude membrane fraction from *X. laevis* oocytes expressing each of the three paralogs (Fig. 2C). The antibody developed against Aqp8aa1shares 12 out of 15 amino acids with the preliminary Aqp8aa2 sequence, so the antibody may very well bind to both proteins. Pre-adsorption of the antibodies with up to 100-fold molar excess of the respective antigenic peptide abolished binding of the antibody to western blots of oocyte membrane fractions expressing each aquaporin or homogenates from pyloric caeca or liver [data not shown; Aqp8ab antibody validated in Madsen et al. (Madsen et al., 2011)].

Immunoblotting of oocytes and tissues

Total membrane fractions from *X. laevis* oocytes injected with 15 ng of *aqp8aa1*, *aqp8ab* or *aqp8b* cRNA were prepared according to Kamsteeg and Deen (Kamsteeg and Deen, 2001). Ten oocytes, frozen in liquid N_2, were homogenized in HbA buffer [in mmol l^{-1}: 20 Tris-HCl (pH 7.4), 5 $MgCl_2$, 5 NaH_2PO_4, 1 EDTA, 80 sucrose and 1% v/v of a protease inhibitor cocktail (P8340, Sigma-Aldrich)] using a P200 pipette and subsequently centrifuged for 5 min at 200 ***g*** at 4°C. The supernatant from this step was centrifuged again under the same conditions and the resulting supernatant was centrifuged for 20 min at 20,000 ***g*** to pellet a total membrane preparation. The pellet was resuspended in 1× NuPAGE LDS sample buffer (Invitrogen, Carlsbad, CA, USA) in a volume of 0.33 oocytes μl^{-1}.

Liver or intestinal tissue were homogenized in SEI buffer pH 7.3 [in mmol l^{-1}: 300 sucrose, 20 Na_2EDTA, 50 imidazole, 1% v/v of a protease inhibitor cocktail (P8340, Sigma-Aldrich)] with a tight-fitting glass mortar and pestle, followed by centrifugation at 2000 ***g*** for 10 min at 4°C. The supernatant was then recentrifuged for 30 min at 50,000 ***g*** to pellet an enriched plasma membrane fraction. The pellet was resuspended in 1× NuPAGE LDS sample buffer in a concentration of 5 µg μl^{-1}. SDS PAGE and electro-blotting was performed using the NuPAGE system (Invitrogen) according to the manufacturer's instructions. Fifty micrograms of liver or intestinal protein or 3.3 oocytes were loaded per lane and separated by 200 V for 35 min using a 2-(*N*-morpholino)ethanesulfonic acid (MES) running buffer (Invitrogen). Proteins were then blotted onto a nitrocellulose or PVDF membrane using a tris-glycine transfer buffer (in mmol l^{-1}: 7.5 Tris, 60 glycine 20% v/v methanol) for 2 h at a constant 25 V. Membranes were blocked for 1 h at room temperature in 2% BSA in tris-buffered saline containing Tween 20 [TBS-T; in mmol l^{-1}: 20 Tris, 140 NaCl, 1% Tween 20). Primary antibodies (Rabbit IgG anti Aqp8aa1, Aqp8ab or Aqp8b (all 2.5 µg ml^{-1})] and mouse anti β-actin (0.25 µg ml^{-1}; Abcam, Cambridge, UK) were diluted in TBS-T containing 2% BSA and incubated overnight at 4°C. Membranes were washed four times 5 min in TBS-T and incubated in TBS-T and 2% BSA with goat-anti rabbit and goat-anti mouse IgG secondary antibodies conjugated to the fluorophores Cy5 and Cy3, respectively (Invitrogen), for 1 h at room temperature. The membrane was then washed four more times in TBS-T and allowed to dry overnight before being scanned with a Typhoon Trio Variable mode Imager (GE Healthcare, Little Chalfont, UK). Relative measurements of protein abundance were performed with the ImageJ gel analyzer tool (http://rsbweb.nih.gov/ij/docs/menus/analyze.html#gels) and β-actin was used for normalization of protein abundance.

Immunofluorescence of oocytes and tissue sections

Tissues were dissected out of the SW-acclimated fish and immediately fixed in 4% paraformaldehyde (4% PFA, 0.9% NaCl, 5 mmol l^{-1} NaH_2PO_4, pH 7.4) overnight at 4°C. They were then washed repeatedly in 70% EtOH before being transferred through increasing concentrations of EtOH to xylene and embedded in paraffin blocks. Tissue sections were cut to a thickness of 5 µm and heated at 55°C (oocytes at 37°C overnight) for 2 h before being hydrated through decreasing concentrations of EtOH. Tissue sections were demasked by boiling in Tris EDTA buffer (in mmol l^{-1}: 10 Tris, 1 EDTA, 0.05% Tween-20) for 10 min and left to cool for 30 min at room temperature. Oocytes did not undergo antigen

retrieval. After one wash in PBS (in mmol l^{-1} 137 NaCl, 2.7 KCl, 1.5 KH_2PO_4, 4.3 Na_2HPO_4, pH 7.3), sections were blocked for 30 min in PBS-T (PBS, 0.05% Tween-20) containing 5% normal goat serum and 0.1% BSA. They were then incubated overnight at 4°C with a cocktail of primary antibodies against one of the salmon Aqp8 paralogs (Rabbit IgG 1–5 μg ml^{-1}) and against the alpha subunit of the Na^+/K^+-ATPase (mouse IgG α5 0.5 μg ml^{-1}; Developmental Studies Hybridoma Bank developed under auspices of the National Institute of Child Health Development and maintained by The University of Iowa, Department of Biological Sciences, Iowa City, IA, USA). After four washes in PBS-T, sections were incubated for 1 h at room temperature with secondary antibodies (4 μg ml^{-1}) goat anti mouse IgG Alexa Fluor 568 and goat anti rabbit IgG Oregon Green 488 (Invitrogen). Sections were washed four times in PBS-T and in some cases after the second wash incubated for 5 min with 0.1 μg ml^{-1} of 4′,6-diamidino-2-phenylindole (DAPI) in PBS to stain the nuclei of the cells. Sections were then washed twice in PBS-T followed by a wash in dH_2O before being allowed to dry. Coverslips were mounted on the slides with ProLong Gold antifade reagent (Invitrogen). Stained tissues were inspected with a Leica HC microscope (Leica Microsystems, Wetzlar, Germany) and representative pictures were obtained with a Leica DC200 camera. Confocal microscopy was performed with a Zeiss LSM510 META confocal microscope (Carl Zeiss, Oberkochen, Germany).

Immunoelectron microscopy

Intestinal samples were isolated from three rainbow trout and fixed in 4% neutral buffered PFA overnight at 4°C. Tissue blocks of the middle intestine were dissected from the remaining intestine and infiltrated for 2 h with 2.3 mol l^{-1} sucrose in 10 mmol l^{-1} PBS, mounted on holders and rapidly frozen in liquid nitrogen. Ultrathin cryosections (80 nm) were cut on an ultra-cryomicrotome (Reichert Ultracut S, Leica Microsystems, Vienna, Austria) and pre-incubated in 10 mmol l^{-1} PBS with 0.1% skimmed milk powder and 50 mmol l^{-1} glycine. The sections were incubated overnight at 4°C with Aqp8ab or Aqp8b serum diluted in 10 mmol l^{-1} PBS containing 0.1% skimmed milk powder. The primary antibodies were visualized by incubation for 1 h at room temperature with secondary goat anti-rabbit IgG conjugated to 10 nm colloidal gold particles (GAR.EM10, Bio-Cell Research Laboratories, Cardiff, UK; dilution: 1:50) diluted in PBS with 0.1% skimmed milk powder, 0.06% polyethyleneglycol and 1% fish gelatin. Electron micrographs were taken on a Morgagni 268D FEI electron microscope (FEI, Eindhoven, The Netherlands).

Statistics

All statistical comparisons were performed using GraphPad Prism v5.02 (GraphPad Software, La Jolla, CA, USA). Data were analyzed *via* one-way or two-way ANOVA where appropriate followed by Tukey's (one-way ANOVA) or Bonferroni's (two-way ANOA) multiple comparisons *post hoc* test if they showed a Gaussian distribution. If transformation of the data did not result in a Gaussian distribution, a non-parametric Kruskal–Wallis test was performed with a Dunn's *post hoc* test to compare data sets. Data were adjusted for outliers using Grubbs' test. Values are reported as means ± s.e.m.

RESULTS

Cloning and phylogeny of Atlantic salmon aqp8 paralogs

Three full-length cDNAs ranging in length from 798 to 859 bp were isolated from intestinal and hepatic tissues of Atlantic salmon. Each cDNA contained open reading frames of 780 or 798 bp, and encoded proteins of 259 or 265 amino acids, respectively. Alignment of the deduced amino acids and Bayesian inference of the codons and proteins in relation to other teleost *aqp8* orthologs revealed that each Atlantic salmon paralog clustered as one of the three major classes of *aqp8* found in zebrafish (Fig. 1; see supplementary material Table S1 for accession numbers). Within each subcluster, however, the topology of transcripts and proteins closely reflected the expected phylogenetic rank, where the Atlantic salmon sequences clustered together with other salmonids. These data revealed that two *aqp8aa* genes appear to exist in Atlantic salmon that are 92% identical based on preliminary data from the salmon genome for *aqp8aa2*. The longest sequence was *aqp8aa1* (accession no. KC626878), which encoded the 265 amino acid protein with an estimated molecular mass of 27.1 kDa, while the two shorter open reading frames encoded the Aqp8ab (KC626879) and Aqp8b (KC626880) proteins with estimated molecular masses of 27.5 and 27.3 kDa, respectively. Maximum likelihood analyses of the codon alignment confirmed the topology determined *via* Bayesian inference (data not shown). Comparison of the three Atlantic salmon and zebrafish Aqp8 orthologs showed high rates of amino acid substitution (37–39%) for the Aqp8aa1 and Aqp8b proteins, but only 25% for the Aqp8ab proteins. As noted previously for zebrafish (Finn and Cerdà, 2011), each Atlantic salmon paralog retains a long N terminus, a short C terminus and the six transmembrane-spanning domains that are typical of the aquaporin superfamily. In contrast to the Aqp8aa1 paralog, which encodes a canonical NPA motif on hemihelix 3, the Aqp8ab and Aqp8b paralogs harbor non-canonical NPP motifs in this position. Inspection of other teleost Aqp8ab orthologs revealed that each retained the NPP motif on hemihelix 3, while the Aqp8b orthologs were more variable with either a Pro in the third position as found in Atlantic salmon, a Thr in flatfishes such as Atlantic halibut (*Hippoglossus hippoglossus*) and European flounder (*Platichthys flesus*), or a Ser as found in zebrafish.

Functional characterization of salmon aquaporin 8 paralogs

Immunofluorescence microscopy and western blotting of membrane fractions of *X. laevis* oocytes expressing the salmon Aqp8s showed that all three paralogs were translated and translocated to the oocyte plasma membrane and thus able to regulate the permeability of the oocyte (Fig. 2A,C). Accordingly, oocytes expressing Aqp8aa1, -8ab and -8b showed an ~30-, ~19- and ~17-fold increase in P_f, respectively, with respect to the control oocytes, which was inhibited with mercury and partially reversed with β-mercaptoethanol only in the case of Aqp8ab (Fig. 2B). The three salmon Aqp8 paralogs were permeable to urea, but interestingly Aqp8ab and -8b also appeared to transport significant amounts of glycerol (Fig. 2B). The observed molecular weights of the Atlantic salmon Aqp8 paralogs in *X. laevis* oocyte membrane fractions were smaller than the theoretical estimates (Fig. 2C). However, when antibodies were used on membrane fractions from intestinal tissue, the major antigenic signal appeared at ~27–28 kDa (Fig. 3D, Aqp8ab and -8b). The antibodies detected high molecular bands >50 kDa in both non-injected oocytes and oocytes injected with salmon Aqp8 cRNA, but this non-specific band was not present in intestinal samples (Fig. 2C *versus* Fig. 3D). However, in intestinal samples a ~38 kDa band was often seen (Fig. 3D). When the antibodies were used for immunofluorescence on non-injected oocytes, only weak autofluorescence was observed (Fig. 2A, Ctrl, representative image).

Tissue screening of salmon aquaporin 8 paralogs

The Atlantic salmon *aqp8* paralogs each had a distinct expression profile in the range of tissues examined in this study. mRNAs of *aqp8aa(1+2)* were found mainly in the liver (Fig. 3A), but also at

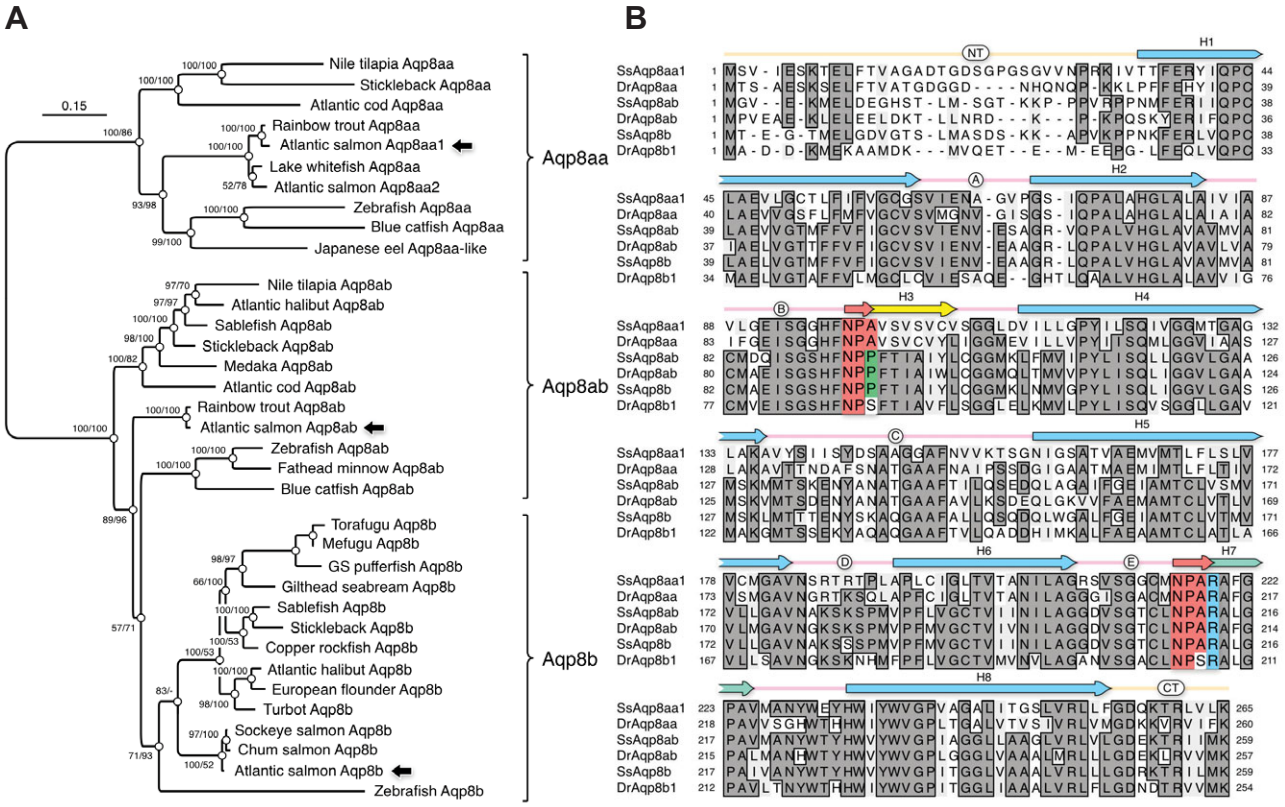

Fig. 1. Molecular phylogeny of Atlantic salmon Aqp8 paralogs. (A) Bayesian majority rule consensus tree of the codon alignment. The tree is midpoint rooted. Posterior probabilities derived from 5 million Markov chain Monte Carlo generations of the codon/amino acid alignments are shown at each node. Scale bar represents the rate of nucleotide substitution per site. (B) Multiple sequence alignment of the Atlantic salmon (Ss) and zebrafish (Dr) Aqp8 paralogs highlighting the N termini (NT), the five loops (A–E), the helical domains (H1–8) and the C termini (CT). Fully conserved residues are boxed and shaded dark grey, while residues with similar chemical properties are shaded light grey.

basal levels in nearly all other tissues examined, except for the brain, which showed slightly higher expression levels. mRNAs of *aqp8ab* were expressed exclusively in the intestinal segments and the spleen (Fig. 3C), while *aqp8b* mRNAs were expressed at varying levels in all tested tissues (Fig. 3E). The most prominent *aqp8b* expression was found in the brain, but significant expression was also detected in osmoregulatory tissues such as the esophagus, intestine, kidney and gill. When comparing two long-term SW-acclimated salmon with two FW-acclimated salmon (Fig. 3D,F), *aqp8ab* mRNA (Fig. 3D) but not *aqp8b* mRNA (Fig. 3F) tended to be higher in the intestinal tissues of SW-acclimated salmon. Protein expression levels of Aqp8ab were accordingly high for Aqp8ab in 7 day SW-acclimated fish (Fig. 3B, lane a, see also Fig. 6) but low in sham-transferred fish (Fig. 3B, lane b), whereas it did not change for Aqp8b (Fig. 3B, lanes c,d). In the spleen there was a remarkably higher level of mRNA from both paralogs in SW-acclimated salmon even though the low sample size eliminated statistical comparisons (Fig. 3D,F).

Cellular and subcellular localisation of salmon aquaporin 8 proteins

Aqp8aa(1+2) was localized in intracellular compartments of enterocytes of the middle intestine, where staining was sub-apical below the brush border (Fig. 4A, inset). Aqp8aa(1+2) was also found in hepatocytes of the salmon liver, where staining appeared in a granular pattern reminiscent of cytosolic vesicles (Fig. 4B). In the intestine, Aqp8ab was abundant in the enterocyte brush border in both the middle and posterior intestine with some occasional staining of the basolateral plasma membrane domains of the enterocytes, where it co-localized with the alpha subunit of the Na^+/K^+-ATPase (Fig. 4D,E, yellow staining). Aqp8b was found in the brush border membrane of the middle and posterior intestine (Fig. 4G,H). This protein was present in goblet cells of the middle intestine (Fig. 4G) but was also found at subapical locations throughout the intestinal tissue (Fig. 4G,H). Pre-immune serum for each antibody showed no specific staining of the intestine but only a weak autofluorescence (Fig. 4C,F,I). To eliminate the possibility that the brush border staining observed for Aqp8ab and -8b was due to non-specific binding of the primary antibody to the glycocalyx, a control experiment using immunoelectron microscopy was performed on the closely related rainbow trout. Immunoelectron microscopy of the middle intestine of rainbow trout revealed abundant Aqp8ab and Aqp8b labeling of the apical plasma membrane (brush border) as well as labeling of intracellular vesicles located subapically in the enterocytes (Fig. 5).

Time-course changes in protein expression of Aqp8ab and -8b in intestinal segments

The abundance of the ~28 kDa Aqp8ab protein band in intestinal tissues significantly increased in response to SW transfer (Fig. 6A,C). Seven days after SW transfer the abundance of Aqp8ab was significantly higher in membrane fractions from pyloric caeca and the middle intestine of SW-transferred individuals compared with sham-transferred fish. There was a significant interaction between time and SW on Aqp8ab expression in both tissues tested. High proteolytic activity in samples from the posterior intestine made it

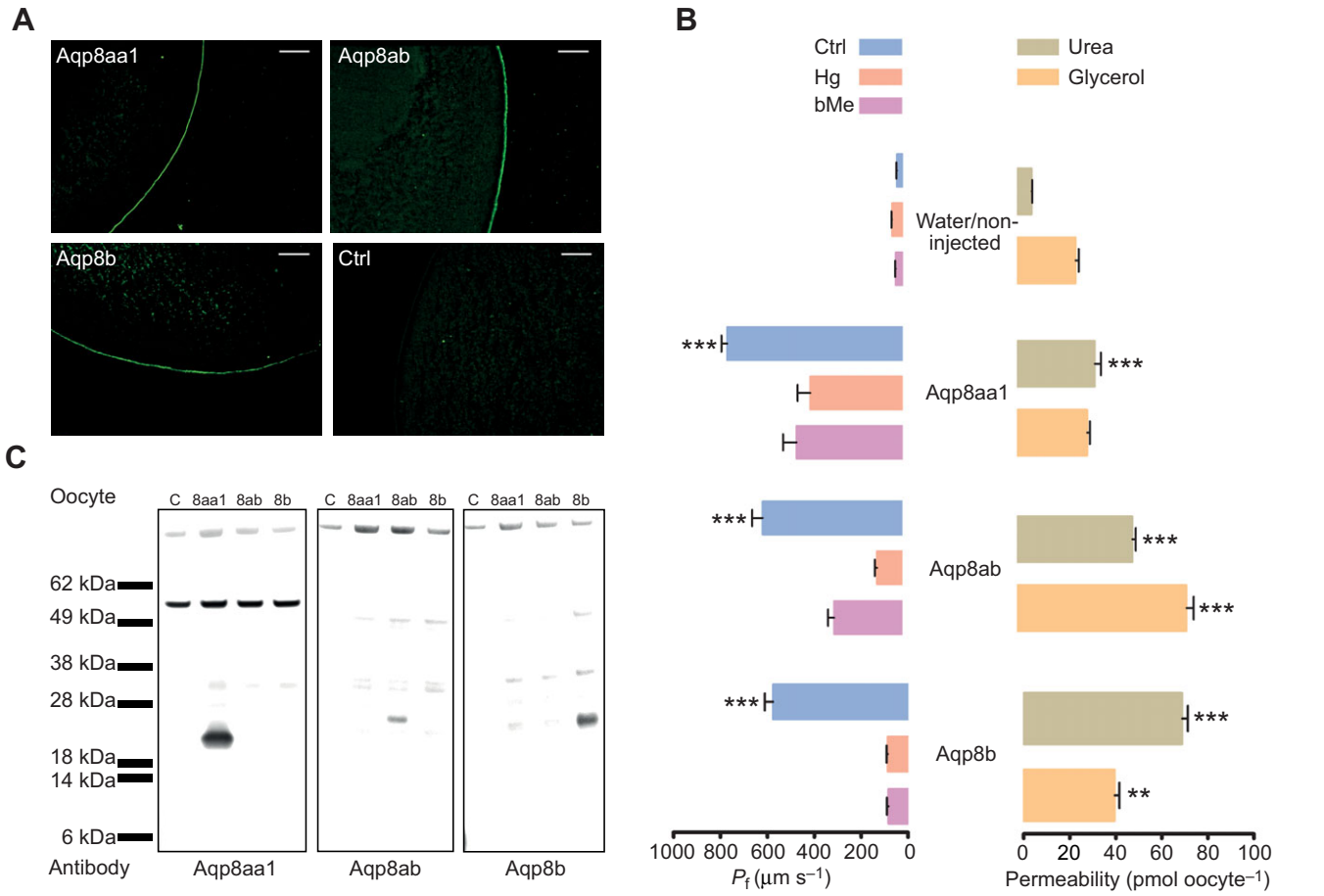

Fig. 2. (A) Immunofluorescence micrographs of *Xenopus laevis* oocytes expressing salmon aquaporin 8 paralogs and a non-injected control oocyte probed with one of the salmon Aqp antibodies (representative image). Scale bars, 50 μm. (B) Relative permeability to water (left panel), urea and glycerol (right panel) of *X. laevis* oocytes expressing salmon aquaporin 8 paralogs. Left: non-injected oocytes or oocytes injected with cRNA corresponding to Aqp8aa1, Aqp8ab or Aqp8b subjected to swelling assays without further treatment (Ctrl) or subjected to 0.1 mmol l^{-1} HgCl (Hg) and in some cases followed by 5 mmol l^{-1} β-mercaptoethanol (bMe) to test for recovery prior to swelling assay. Asterisks indicate significant difference in relative water permeability between non-injected and control oocytes (***P<0.001). Right: radioactive uptake of [^{3}H] glycerol or [^{14}C] urea by water-injected oocytes or oocytes injected with cRNA as explained above. Asterisks indicate significant difference from water-injected oocytes (**P<0.01, ***P<0.001). Presented data are from one representative experiment and shown as means ± s.e.m., N=12–20. (C) Immunoblots of membrane fractions from *X. laevis* oocytes expressing Aqp8aa1, Aqp8ab or Aqp8b. Each antibody was probed against an enriched membrane fraction from oocytes expressing one of the three salmon aquaporin 8 paralogs or from control (C) oocytes. Molecular weight marker is shown on the left side.

impossible to probe for changes in Aqp8ab and Aqp8b protein expression in this segment. Some truncated protein fragments between 10 and 14 kDa were detected by the Aqp8ab antibody in some intestinal samples from both SW- and FW-acclimated fish (Fig. 6E). A reaction with the Aqp8ab antibody was also seen around 38 kDa in samples with high abundance of the 28 kDa protein, possibly reflecting a glycosylated form of the aquaporin (Fig. 6E). The abundance of the ~27 kDa Aqp8b protein did not change significantly in membrane fractions from pyloric caeca or the middle intestine during 7 days of SW acclimation, and the variation in protein abundance was high in both SW-acclimated fish and sham-transferred fish (Fig. 6B,C,F). Time-course changes in Aqp8aa(1+2) protein expression were not investigated because of its low abundance in membrane fractions from intestinal tissues, possibly because of its intracellular localization. Hence, it was a less obvious candidate for transcellular water transport.

DISCUSSION

AQP8 is a versatile transmembrane channel expressed in multiple tissues of different mammals where it has been suggested to be involved in the maintenance of intracellular osmotic equilibrium, transport of ammonia and small organic solutes or mitochondrial expansion during oxidative phosphorylation (Elkjær et al., 2001; Calamita et al., 2005; Saparov et al., 2007). In contrast to mammals, in which only a single *AQP8* gene is known, the multiplicity of Aqp8 paralogs in fish offers a possibility of dissecting the evolutionary form and function of a closely related set of genes. The present study adds knowledge to the puzzle of Aqp8 evolution initiated recently through studies on zebrafish (Tingaud-Sequeira et al., 2010; Cerdà and Finn, 2010; Finn and Cerdà, 2011). We extend the available information by identifying novel transport properties of two Aqp8 paralogs in Atlantic salmon and show for the first time that the expression of Aqp8ab channels, which are located in the brush border of enterocytes, is upregulated in response to SW acclimation.

Phylogenetic analysis of salmon aquaporin 8 paralogs

The Bayesian analyses clearly show that the Atlantic salmon *aqp8* paralogs isolated in the present study are representatives of the three major classes of *aqp8* genes originally identified and characterized

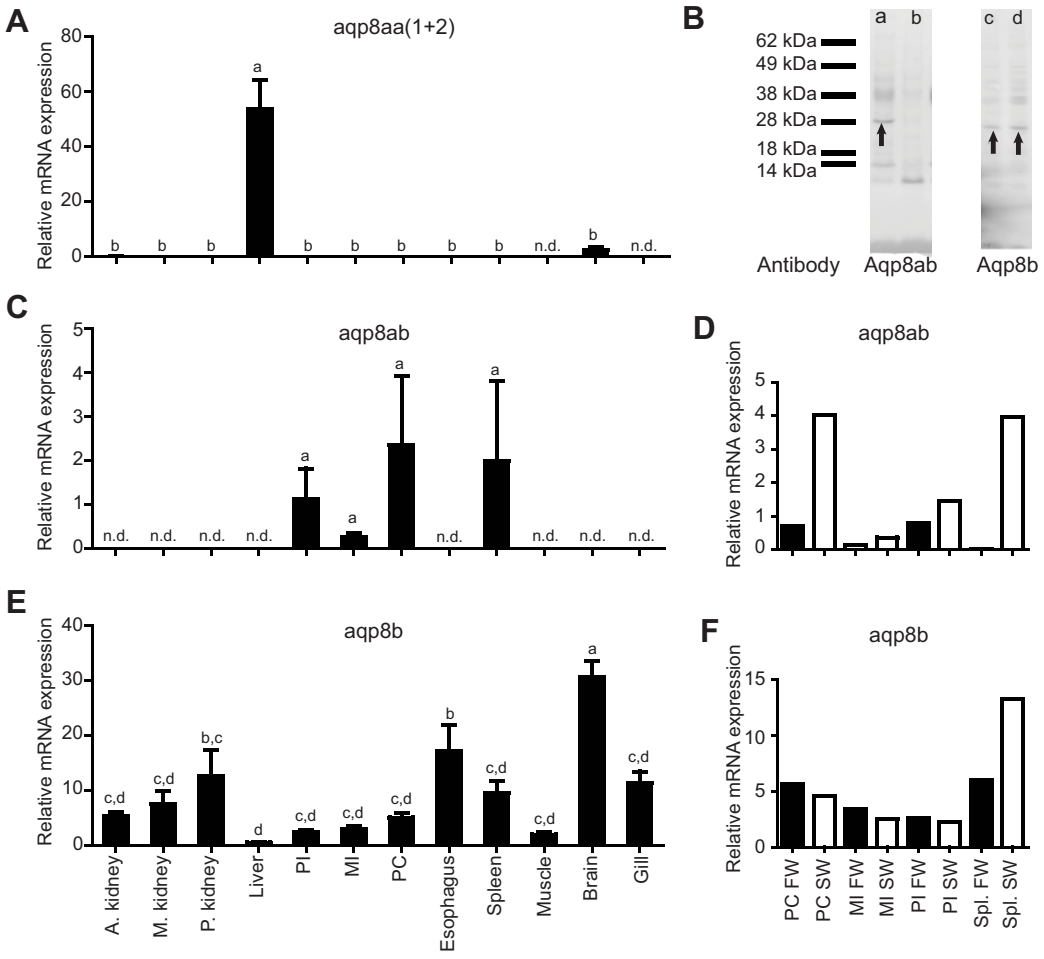

Fig. 3. (A,C,E) Tissue mRNA expression patterns of three Atlantic salmon *aqp8* paralogs. Tissues are shown in E. A., M. and P. kidney, anterior, middle and posterior kidney. mRNA expression is measured relative to *ef1a* and data are shown as means ± s.e.m., *N*=4, representing two seawater (SW)-acclimated and two freshwater (FW)-acclimated salmon. n.d., not detected. Different letters indicate significant differences between tissue expression levels in each panel ($P<0.05$). (B) Immunoblots of membrane fractions from pyloric caeca of 7 day SW-acclimated salmon (a,d) and 7 day sham-transferred FW salmon (b,c) probed with antibodies against Aqp8ab (a,b) or Aqp8b (c,d). Arrows point to native Aqp protein bands. Molecular weight marker is shown on the left side. (D,F) mRNA expression patterns in relation to osmotic environment of *aqp8ab* and *-8b* in intestinal tissue and spleen (shown in F). PC, pyloric caeca; MI, middle intestine; PI, posterior intestine, Spl., spleen. Data are shown as means (*N*=2).

in zebrafish (Tingaud-Sequeira et al., 2010). The present observation that the subcluster topology closely follows the phylogenetic rank of each species and that each paralog retains conserved features, such as the canonical and non-canonical NPA motifs, is consistent with an early diversification of the *aqp8* genes during fish evolution (Cerdà and Finn, 2010; Finn and Cerdà, 2011). This became evident when the genomic synteny of the different paralogs was examined, revealing that *aqp8aa* and *aqp8ab* are closely linked in distantly related teleost genomes whereas *aqp8b* is located on a different chromosome (Cerdà and Finn, 2010). The presence of a second *aqp8aa* gene reported here for Atlantic salmon is potentially consistent with the occurrence of a fourth round of genome duplication in the salmonid lineage (Moghadam et al., 2011).

Functional characteristics of salmon aquaporin 8 paralogs

The permeability properties of mammalian AQP8 have been under dispute for some years, as studies of human, rat and mouse AQP8 using *X. laevis* oocytes or reconstituted liposomes have led to different conclusions. All studies show that AQP8 is water permeable, but its ability to also transport small solutes such as urea is controversial (Liu et al., 2006; Yang et al., 2006). The three salmon aquaporin paralogs were successfully translated in *X. laevis* oocytes and the protein products transported to the plasma membrane, as demonstrated by western blotting of enriched membrane fractions and immunofluorescence microscopy. All paralogs showed significant water permeability, as expected from studies performed on mammalian AQP8 channels (Liu et al., 2006; Yang et al., 2006; Saparov et al., 2007). The significant urea permeability of all three paralogs corresponds well with the fact that two out of three zebrafish paralogs [Aqp8aa and Aqp8ab (Tingaud-Sequeira et al., 2010)] and the murine AQP8 ortholog (Ma et al., 1997) are also permeable to urea. Rat and human AQP8, however, do not seem to be urea permeable (Liu et al., 2006). Glycerol permeability has not been reported for any vertebrate Aqp8 ortholog, but this study shows that two of the Atlantic salmon paralogs, Aqp8ab and -8b, are significantly permeable to glycerol. It is somewhat surprising that the liver paralog Aqp8aa1 did not show glycerol permeability, as glycerol metabolism in this organ is of major importance. Aqp8aa2, which was not cloned and expressed in *X. laevis* oocytes, is suspected to function similarly as Aqp8aa1 because of their high degree of identical amino acid residues. The intestinal paralog Aqp8ab showed the highest glycerol permeability, perhaps suggesting a role of this aquaporin in glycerol mobilization in addition to water transport.

Tissue-specific expression of aqp8 paralogs

The tissue expression profile for Atlantic salmon *aqp8aa(1+2)* mRNA reported here is consistent with that of the *aqp8aa2* gene [formerly annotated as *aqp8a* (Tipsmark et al., 2010)], which was highly expressed in the liver. The study by Tipsmark et al. (Tipsmark et al., 2010) may also have amplified *aqp8aa1* mRNA as the primers used then were the same as in the present study and they are unable to distinguish between the two paralogs. The *aqp8aa1* paralog was cloned from the liver and thus is expressed in this tissue to some degree. Because of the high similarity between the two *aqp8aa* paralogs in comparison with the other *aqp8* paralogs in salmon, one might expect them still to be expressed in the same tissues.

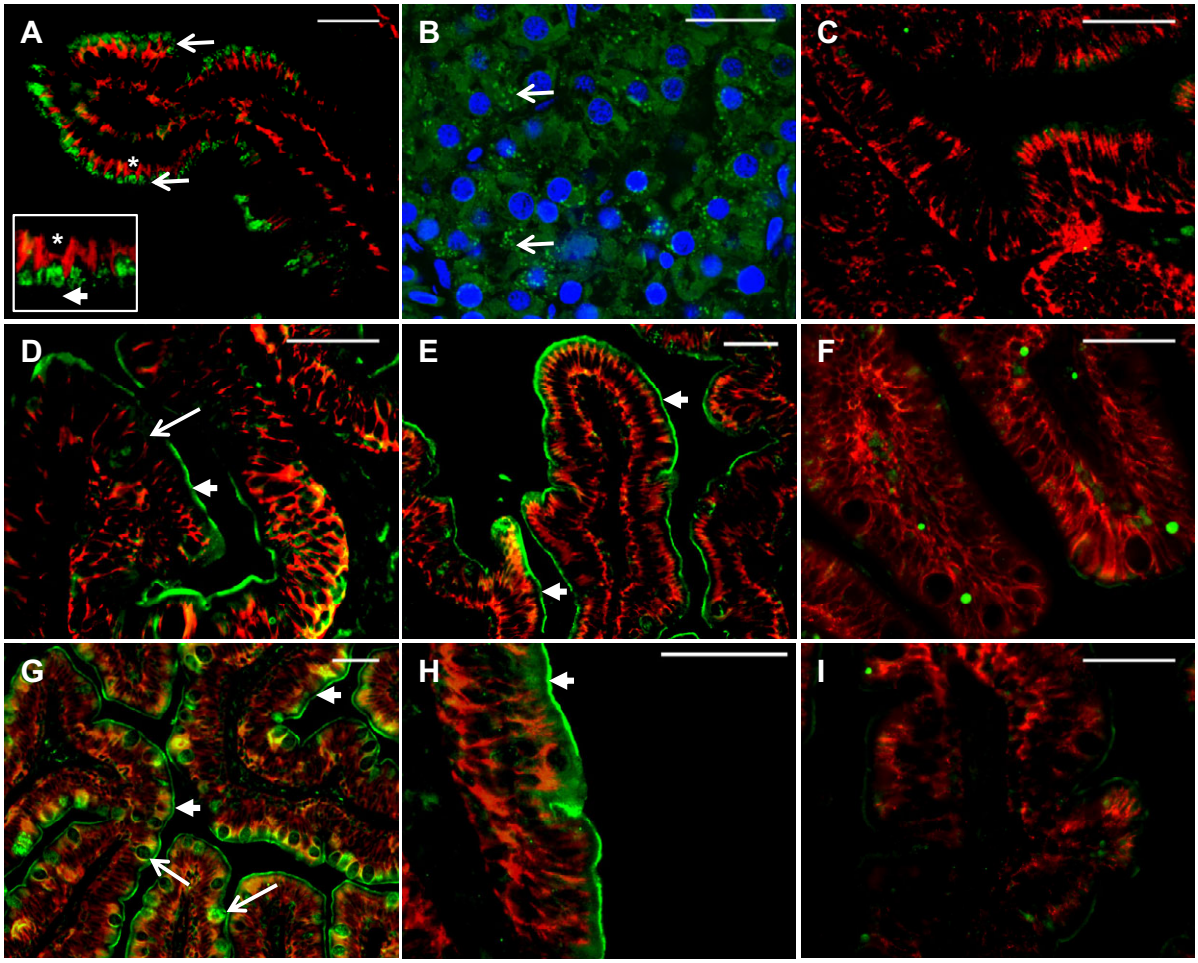

Fig. 4. Immunofluorescence micrographs of salmon aquaporin 8 paralogs in SW-acclimated salmon. (A) Aqp8aa(1+2) (green) and the alpha subunit of the Na^+/K^+-ATPase (red) in middle intestine. Inset: sub-apical localization of Aqp8aa(1+2). (B) Aqp8aa(1+2) (green) in hepatic tissue, nuclei are counterstained with DAPI (blue). (C,F,I) Pre-immune serum (green) for Aqp8aa(1+2) (C), Aqp8ab (F) and Aqp8b (I) and the alpha subunit of the Na^+/K^+-ATPase (red) in middle intestine. (D,E,G,H) Aqp8ab (D,E) (green) and Aqp8b (G,H) (green) and the alpha subunit of the Na^+/K^+-ATPase (red) in middle intestine (D,G) and posterior intestine (E,H). Asterisks in A and inset show enlarged area. Short arrows (open arrowheads) in A and B point to intracellular locations of Aqp8aa(1+2). Very short arrows (filled arrowheads) in A inset, D, E, G and H point to the approximate location of the brush border membrane of the intestinal epithelium. Long arrows (open arrowheads) in D and G mark goblet cells. Scale bars: A and C–I, 50 μm; B, 25 μm.

However, as is seen with *aqp8* in several teleosts, the expression patterns of the paralogs are highly dynamic and may be subjected to selection early on after a genomic duplication event. A final answer to the evolutionary kinship between *aqp8aa1* and *aqp8aa2* and the relative abundance of the two paralogs awaits further investigation, which will be more interesting from an evolutionary perspective than an osmoregulatory one. The tissue expression profile of the Atlantic salmon *aqp8ab* gene is more similar to that reported for the zebrafish *aqp8ab* gene (Tingaud-Sequeira et al., 2010). The presence of *aqp8* mRNAs in intestinal segments has been observed earlier in different teleosts, although the particular paralog expressed varies between species. For example, eels may express the *aqp8aa* paralog (Cutler et al., 2009; Kim et al., 2010), zebrafish express both the *aqp8aa* and *-8ab* paralogs (Tingaud-Sequeira et al., 2010), while Atlantic salmon expresses the *aqp8ab* and *-8b* paralogs (Tipsmark et al., 2010; present study). In Atlantic salmon, *aqp8ab* mRNA was also present in the spleen, where its apparent upregulation in SW-acclimated animals has not been reported previously. This expression must take place in the splenic tissue itself and not in the abundant blood cells, as a screening of mixed blood cells from the closely related rainbow trout did not reveal any expression of *aqp8ab* mRNA (M.B.E., unpublished observations). There are as yet no other reports of Aqp8 expression in the teleost spleen. The intestinal levels of *aqp8ab* mRNA tended to be elevated in long-term SW-acclimated animals, which is consistent with earlier findings (Cutler et al., 2009; Kim et al., 2010; Tipsmark et al., 2010). In contrast to the tandemly duplicated *aqp8aa1* and *-8ab* transcripts, expression of *aqp8b* is more ubiquitous, with the highest expression levels occurring in the brain. The earlier study in zebrafish (Tingaud-Sequeira et al., 2010) only found expression of *aqp8b* mRNA in the brain, thus the expression of this paralog seems to be highly species specific. As noted for *aqp8ab*, there seemed to be a higher expression of *aqp8b* in the spleen upon SW acclimation, which could represent expression in blood cells or in the splenic tissue itself.

Cellular and subcellular localization of salmon aquaporin 8 proteins

Only selected tissues were investigated by immunofluorescence microscopy in this study because of our focus on the role of Aqp8

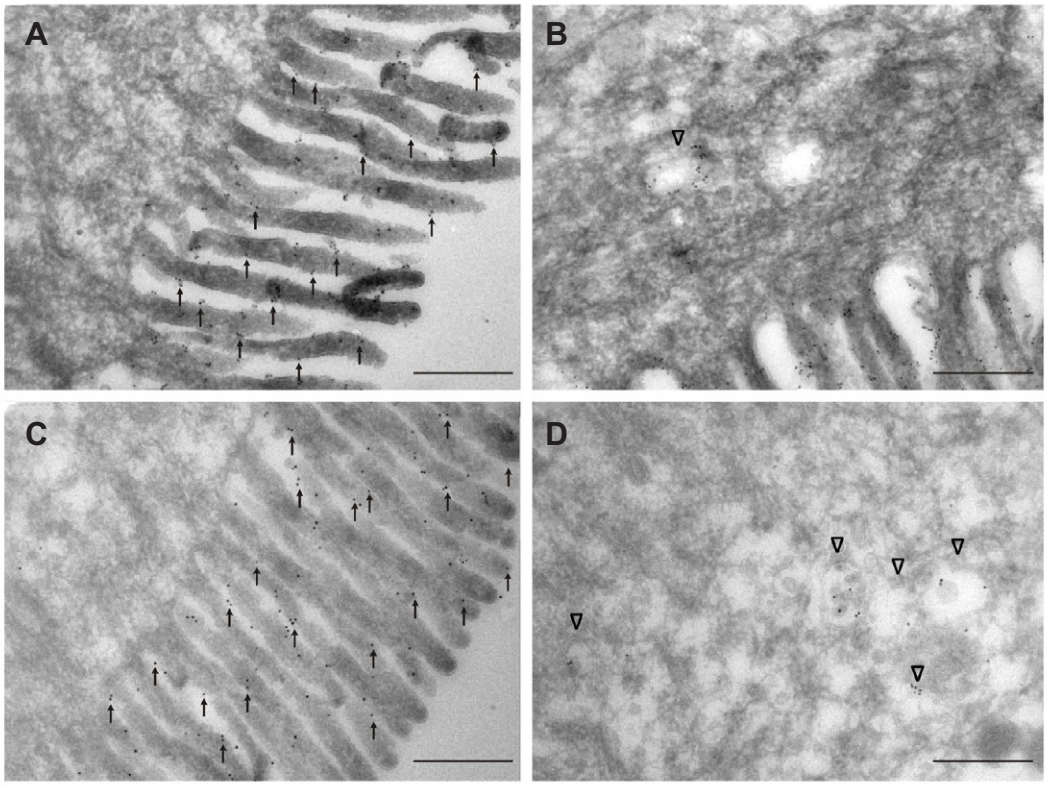

Fig. 5. Immunoelectron micrographs of Aqp8ab (A,B) and Aqp8b (C,D) in the middle intestine of rainbow trout. (A,C) Both Aqp8ab and Aqp8b are abundantly expressed in the apical plasma membrane (brush border) of enterocytes (arrows). (B,D) Expression of Aqp8ab and Aqp8b is also seen in intracellular vesicles located subapically in the cell (arrowheads). Scale bars, 0.5 μm.

in water transport upon SW acclimation. The intracellular immunolocalization of Aqp8aa(1+2) in both the liver and intestine of Atlantic salmon resonates well with earlier findings of AQP8 in mammals. For example, vesicular localization of AQP8 has been reported in rat kidney tubules (Elkjær et al. 2001) and subapical localization in the jejunum and duodenum (Elkjær et al., 2001; Laforenza et al., 2005; Tritto et al., 2007), with intracellular localization noted in colonic enterocytes and hepatocytes (Elkjær et al., 2001). The hepatic vesicular localization in rat was confirmed in a study by García et al. (García et al., 2001), who further demonstrated that cAMP was a strong stimulus for redistribution of the protein to the plasma membrane. Mammalian AQP8 has also been located to the inner mitochondrial membrane of rat hepatocytes (Calamita et al., 2005), where it is proposed to regulate mitochondrial water permeability. The present finding of salmon Aqp8aa(1+2) in the liver is strikingly similar to that reported in rat hepatocytes (Calamita et al., 2005), and seems to correspond to a mitochondrial or vesicular localization for this aquaporin. However, although teleost Aqp8b channels are known to be expressed in mitochondria (Chauvigné et al., 2013), firm conclusions should await further examination of Aqp8aa(1+2) by immunoelectron microscopy.

The brush border membrane localization of both Aqp8ab and -8b in the two salmonid species investigated here supports and extends the hypothesis of Tipsmark et al. (Tipsmark et al., 2010) and Madsen et al. (Madsen et al., 2011) that these aquaporins are important regulators of intestinal transepithelial water transport. The immunoelectron microscopy of Aqp8ab and Aqp8b in the rainbow trout intestine paralleled the findings by immunofluorescence in the intestine of Atlantic salmon. Unpublished observations from our laboratory using immunofluorescence or immunohistochemistry also show similar results in rainbow trout intestine with the Aqp8ab and -8b antibodies. Alignment of a known Aqp8ab from rainbow trout (accession no. CU071568) with the salmon Aqp8ab showed 100% identity at the antibody epitope, and labeling with the Aqp8ab antibody is therefore likely representative of a rainbow trout paralog. The antibody raised against Atlantic salmon Aqp8ab was developed based on EST data (Madsen et al., 2011). Because of a non-synonymous nucleotide polymorphism, there is a single amino acid mismatch at the end of the epitope compared with the cloned paralog and the rainbow trout sequence (T in the antigenic peptide, P in the salmonid paralogs); however, this does not seem to affect the binding of the antibody to the protein. There are currently no available EST data on rainbow trout Aqp8b, but based on the phylogenetic proximity of this species to the Atlantic salmon and the high similarity between Atlantic salmon and rainbow trout Aqp8aa and Aqp8ab proteins, we suspect that there is an Aqp8b paralog expressed in the intestine of rainbow trout with a similar localization as observed for this paralog in Atlantic salmon. The intracellular localization of Aqp8b in the enterocytes and its presence in some goblet cells in the middle intestine suggest that different sorting mechanisms may exist for this and the Aqp8ab protein. Cross-reactivity between the antibodies for the three different paralogs could be a valid concern; however, control experiments using *X. laevis* oocytes showed that cross-reactivity was minimal. Nevertheless, it cannot be excluded that the conformations of the proteins in the fixed intestine are such that cross-reactivity might occur and yield false-positive results. In addition, binding of primary antibodies to glycocalyx is sometimes mistaken as binding of the antibody to apical membrane proteins of intestinal epithelia or other mucous-coated surfaces. However, the immunoelectron microscopy shows that binding of the antibodies to Aqp8ab and -8b in the apical membrane is indeed specific and not an artifact. The intestinal staining pattern of Aqp8ab and Aqp8b agree quite well with previously published results from the rat (Elkjær et al., 2001; Laforenza et al., 2005; Tritto et al., 2007), although the strongest staining in the small intestine of the rat with the AQP8

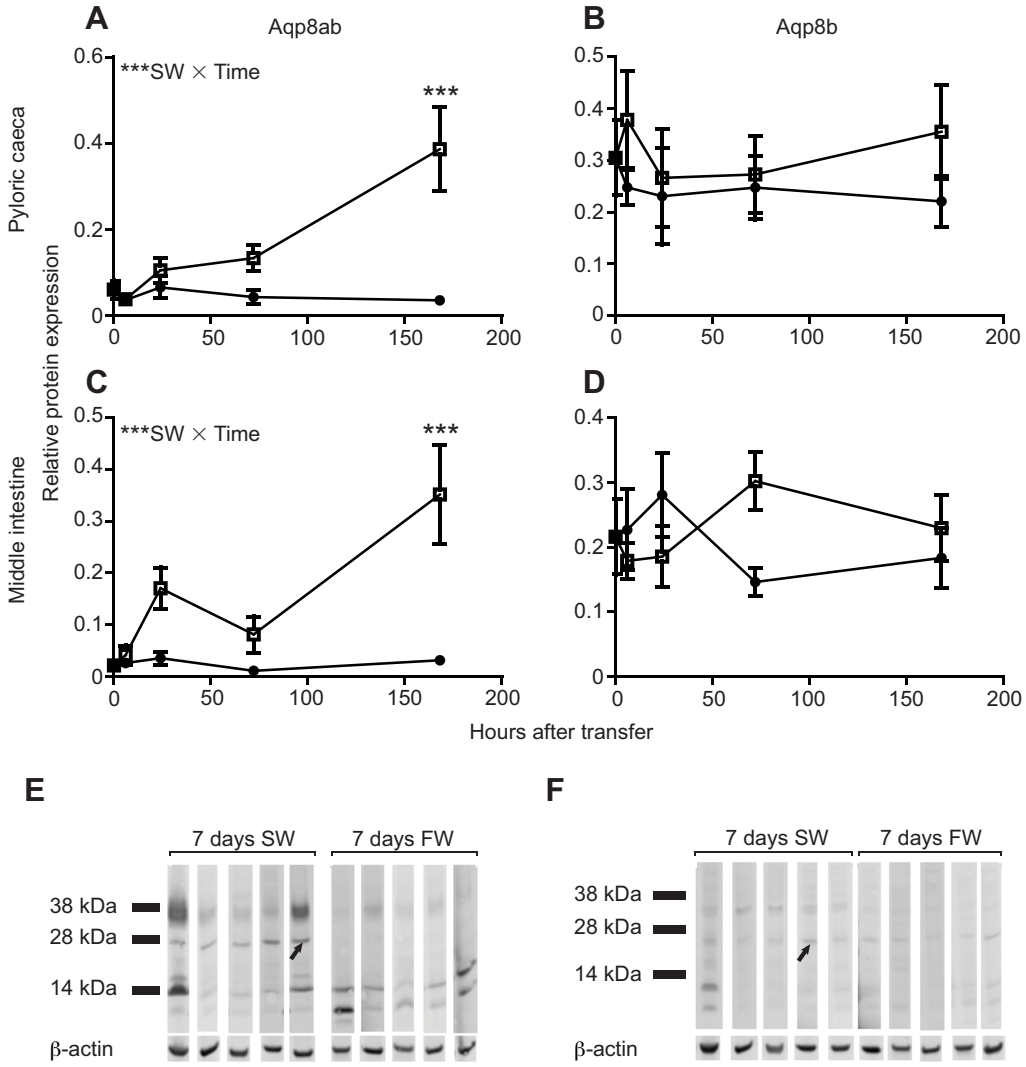

Fig. 6. The effect of SW transfer on Aqp8ab (A,C) and Aqp8b (B,D) protein expression in pyloric caeca (top panels) and middle intestine (lower panels) membrane fractions. Data are normalized with respect to expression levels of β-actin proteins. Open squares represent SW-transferred fish and closed circles represent sham-transferred fish. Significant interactions between time and treatment are indicated by ***SW × time (P<0.001). Asterisks above data points show a significant difference between SW- and sham-transferred fish at that time point (***P<0.001). Data are shown as means ± s.e.m., N=4–6. (E,F) Representative immunoblots of membrane fractions from pyloric caeca of SW-acclimated and sham-transferred salmon. The blots were probed with antibodies against Atlantic salmon Aqp8ab (E) or Aqp8b (F). Arrows point to protein bands used for the semi-quantitative analysis in A–D.

antibody was seen in the sub-apical part of the enterocytes rather than the brush border membrane found here in the salmon intestine. The immunoelectron microscopy also detected Aqp8ab and Aqp8b labeling in subapical vesicular structures. Whether Aqp8 proteins located in these vesicular structures are destined for plasma membrane insertion, degradation or recycling to other cellular compartments is presently unknown and requires closer investigation of marker proteins expressed in the vesicles associated with Aqp8 labeling. Different trafficking mechanisms may be responsible for recruiting the Aqp8 proteins to the intestinal brush border membrane. Trafficking may involve kinase phosphorylation of the proteins, and from this perspective it is interesting to note that Aqp8aa1 and -8b have predicted N-terminal serine phosphorylation residues that are missing in the Aqp8ab protein [*in silico* prediction using NetPhos 2.0 (Blom et al., 1999)]. The role of these residues awaits further investigation.

Effect of SW on protein expression of Aqp8ab and Aqp8b

The increasing intestinal expression of the Aqp8ab protein upon SW challenge supports previous reports of elevated *aqp8* mRNA levels in the intestine of various fish species exposed to SW (Cutler et al., 2009; Tipsmark et al., 2010; Kim et al., 2010). These findings underline the important role of this paralog in transforming the intestine into a water-absorptive organ when fish are exposed to hyperosmotic conditions. In this study, we analyzed protein expression in an enriched plasma membrane fraction, thus suggesting a functional membrane localization of Aqp8ab as observed by immunoelectron microscopy of Aqp8ab in the rainbow trout intestine. The immunoblots revealed bands of higher and lower expected molecular weight than the native Aqp8 proteins. The nature of these bands is unknown at present but might reflect post-translationally modified Aqp8 proteins (e.g. coupled with sugars, ubiquitin, etc.). As suggested by Madsen et al. (Madsen et al., 2011), apical as well as basolateral localization of Aqp8ab may create a regulated transcellular pathway of water movement, which may be supplemented by apical expression of other aquaporin paralogs – especially Aqp1aa (Martinez et al., 2005a; Raldúa et al., 2008; Madsen et al., 2011). Recent experiments using radiolabelled polyethylene glycol molecules in the intestine of killifish (*Fundulus heteroclitus*) have indeed shown that the transcellular route of water absorption is more important than the paracellular route (Wood and Grosell, 2012). Regulation of aquaporin expression in the intestine of fish upon SW challenge could thus prove valuable to the understanding of osmotic homeostasis in the intestine of vertebrates. In contrast to Aqp8ab, immunoblotting did not reveal any regulation of membrane-bound Aqp8b protein or its mRNA upon SW transfer. This protein was localized apically, both in the brush border zone as well as sub-apically in vesicular compartments. The apparent lack

of regulation and the ubiquitous tissue distribution suggest that Aqp8b performs a housekeeping function such as cell volume regulation or is associated with water homeostasis of intracellular compartments. A role in mucus secretion is also suggested by the presence of this paralog in goblet cells.

Conclusions and perspectives

In summary, we have characterized three main classes of Aqp8 in the Atlantic salmon. There appear to be yet more *aqp8* paralogs in the genome of Atlantic salmon as judged from the extra *aqp8aa* paralog, which is consistent with the partial tetraploid status of this species. The paralogs investigated in the present study show divergent expression patterns, which suggests that they perform different functions in the tissues where they are expressed. Aqp8aa(1+2) is the main paralog expressed in the liver and may be involved in maintaining internal osmotic balance in hepatocytes or perhaps be involved in bile fluid formation, but the specific role of each paralog requires further investigation. Our data support a physiological role of Aqp8ab in the transcellular water uptake across intestinal enterocytes upon SW exposure where Aqp8b may play a supporting role. Goblet cell expression of Aqp8b suggests that this protein has a role in mucus production/secretion, as suggested for Aqp1aa [*S. salar* intestine (Madsen et al., 2011)] and Aqp3b [*A. anguilla* rectum (Lignot et al., 2002) and esophagus (Cutler et al., 2007)]. The acquired glycerol permeability of the Aqp8ab and Aqp8b paralogs and their distinct expression profiles suggest that the Atlantic salmon Aqp8 water channels have neofunctionalized. In future studies it will be important to decipher the hormonal and environmental factors that initiate the divergent expression patterns and the structural alterations that facilitated a broader selection of solutes to permeate the channel.

ACKNOWLEDGEMENTS

The staff at the Danish Centre for Wild Salmon is thanked for their help with animal husbandry and seawater challenge experiments. Annette Duus and Else-Merete Løcke are thanked for valuable technical assistance.

AUTHOR CONTRIBUTIONS

M.B.E., B.M.C., J.C., R.N.F., and S.S.M. conceived and designed the experiments. M.B.E., F.C., B.M.C., R.N.F., J.C. and S.S.M. performed the experiments and interpreted the results. M.B.E. drafted the manuscript. M.B.E., F.C., B.M.C., R.N.F., J.C. and S.S.M. edited, revised and approved the manuscript.

COMPETING INTERESTS

No competing interests declared.

FUNDING

This study was supported by grants from the Danish Natural Research Council (09-070689 to S.S.M.), the Spanish Ministry of Science and Innovation (MICINN; AGL2010-15597 to J.C.) and the Research Council of Norway (204813/F20 and 224816/E40 to R.N.F.). B.M.C. was supported by The Danish Council for Independent Research – Medical Sciences and the Lundbeck Foundation, and F.C. was supported by a postdoctoral contract Juan de la Cierva from Spanish MICINN.

REFERENCES

Ando, M., Mukuda, T. and Kozaka, T. (2003). Water metabolism in the eel acclimated to seawater: from mouth to intestine. *Comp. Biochem. Physiol.* **136B**, 621-633.

Beyenbach, K. W. (2004). Kidneys sans glomeruli. *Am. J. Physiol.* **286**, F811-F827.

Blom, N., Gammeltoft, S. and Brunak, S. (1999). Sequence and structure-based prediction of eukaryotic protein phosphorylation sites. *J. Mol. Biol.* **294**, 1351-1362.

Brown, J. A., Jackson, B. A., Oliver, J. A. and Henderson, I. W. (1978). Single nephron filtration rates (SNGFR) in the trout, *Salmo gairdneri*. Validation of the use of ferrocyanide and the effects on environmental salinity. *Pflugers Arch.* **377**, 101-108.

Brown, J. A., Oliver, J. A., Henderson, I. W. and Jackson, B. A. (1980). Angiotensin and single nephron glomerular function in the trout *Salmo gairdneri*. *Am. J. Physiol.* **239**, R509-R514.

Buddington, R. K. and Diamond, J. M. (1987). Pyloric ceca of fish: a 'new' absorptive organ. *Am. J. Physiol.* **252**, G65-G76.

Calamita, G., Ferri, D., Gena, P., Liquori, G. E., Cavalier, A., Thomas, D. and Svelto, M. (2005). The inner mitochondrial membrane has aquaporin-8 water channels and is highly permeable to water. *J. Biol. Chem.* **280**, 17149-17153.

Cerdà, J. and Finn, R. N. (2010). Piscine aquaporins: an overview of recent advances. *J. Exp. Zool.* **313A**, 623-650.

Chauvigné, F., Boj, M., Vilella, S., Finn, R. N. and Cerdà, J. (2013). Subcellular localization of selectively permeable aquaporins in the male germ line of a marine teleost reveals spatial redistribution in activated spermatozoa. *Biol. Reprod.* **89**, 1-17.

Cutler, C. P. and Cramb, G. (2002). Branchial expression of an aquaporin 3 (AQP-3) homologue is downregulated in the European eel *Anguilla anguilla* following seawater acclimation. *J. Exp. Biol.* **205**, 2643-2651.

Cutler, C. P., Martinez, A. S. and Cramb, G. (2007). The role of aquaporin 3 in teleost fish. *Comp. Biochem. Physiol.* **148A**, 82-91.

Cutler, C. P., Philips, C., Hazon, N. and Cramb, G. (2009). Aquaporin 8 (AQP8) intestinal mRNA expression increases in response to salinity acclimation in yellow and silver European eels (*Anguilla anguilla*). *Comp. Biochem. Physiol.* **153A**, S78.

Davidson, W. S., Koop, B. F., Jones, S. J. M., Iturra, P., Vidal, R., Maass, A., Jonassen, I., Lien, S. and Omholt, S. W. (2010). Sequencing the genome of the Atlantic salmon (*Salmo salar*). *Genome Biol.* **11**, 403-409.

Deen, P. M. T., Verdijk, M. A. J., Knoers, N. V., Wieringa, B., Monnens, L. A., van Os, C. H. and van Oost, B. A. (1994). Requirement of human renal water channel aquaporin-2 for vasopressin-dependent concentration of urine. *Science* **264**, 92-95.

Elkjær, M. L., Nejsum, L. N., Gresz, V., Kwon, T. H., Jensen, U. B., Frøkiaer, J. and Nielsen, S. (2001). Immunolocalization of aquaporin-8 in rat kidney, gastrointestinal tract, testis, and airways. *Am. J. Physiol.* **281**, F1047-F1057.

Engelund, M. B. and Madsen, S. S. (2011). The role of aquaporins in the kidney of euryhaline teleosts. *Front. Physiol* **2**, 51.

Evans, D. H., Piermarini, P. M. and Choe, K. P. (2005). The multifunctional fish gill: dominant site of gas exchange, osmoregulation, acid-base regulation, and excretion of nitrogenous waste. *Physiol. Rev.* **85**, 97-177.

Fabra, M., Raldúa, D., Power, D. M., Deen, P. M. T. and Cerdà, J. (2005). Marine fish egg hydration is aquaporin-mediated. *Science* **307**, 545.

Fabra, M., Raldúa, D., Bozzo, M. G., Deen, P. M. T., Lubzens, E. and Cerdà, J. (2006). Yolk proteolysis and aquaporin-1o play essential roles to regulate fish oocyte hydration during meiosis resumption. *Dev. Biol.* **295**, 250-262.

Finn, R. N. and Cerdà, J. (2011). Aquaporin evolution in fishes. *Front. Physiol.* **2**, 44.

García, F., Kierbel, A., Larocca, M. C., Gradilone, S. A., Splinter, P., LaRusso, N. F. and Marinelli, R. A. (2001). The water channel aquaporin-8 is mainly intracellular in rat hepatocytes, and its plasma membrane insertion is stimulated by cyclic AMP. *J. Biol. Chem.* **276**, 12147-12152.

Grosell, M., O'Donnell, M. J. and Wood, C. M. (2000). Hepatic versus gallbladder bile composition: in vivo transport physiology of the gallbladder in rainbow trout. *Am. J. Physiol.* **278**, R1674-R1684.

Hiroi, J., McCormick, S. D., Ohtani-Kaneko, R. and Kaneko, T. (2005). Functional classification of mitochondrion-rich cells in euryhaline Mozambique tilapia (*Oreochromis mossambicus*) embryos, by means of triple immunofluorescence staining for Na^+/K^+-ATPase, $Na^+/K^+/2Cl^-$ cotransporter and CFTR anion channel. *J. Exp. Biol.* **208**, 2023-2036.

Hwang, P. P., Lee, T. H. and Lin, L. Y. (2011). Ion regulation in fish gills: recent progress in the cellular and molecular mechanisms. *Am. J. Physiol.* **301**, R28-R47.

Kamsteeg, E. J. and Deen, P. M. (2001). Detection of aquaporin-2 in the plasma membranes of oocytes: a novel isolation method with improved yield and purity. *Biochem. Biophys. Res. Commun.* **282**, 683-690.

Karnaky, K. J. (1986). Structure and function of the chloride cell of *Fundulus heteroclitus* and other teleosts. *Am. Zool.* **26**, 209-224.

Katoh, K. and Toh, H. (2008). Recent developments in the MAFFT multiple sequence alignment program. *Brief. Bioinform.* **9**, 286-298.

Kim, Y. K., Watanabe, S., Kaneko, T., Do Huh, M. and Park, S. I. (2010). Expression of aquaporins 3, 8 and 10 in the intestines of freshwater- and seawater-acclimated Japanese eels *Anguilla japonica*. *Fish. Sci.* **76**, 695-702.

Laforenza, U., Cova, E., Gastaldi, G., Tritto, S., Grazioli, M., LaRusso, N. F., Splinter, P. L., D'Adamo, P., Tosco, M. and Ventura, U. (2005). Aquaporin-8 is involved in water transport in isolated superficial colonocytes from rat proximal colon. *J. Nutr.* **135**, 2329-2336.

Lignot, J. H., Cutler, C. P., Hazon, N. and Cramb, G. (2002). Immunolocalisation of aquaporin 3 in the gill and the gastrointestinal tract of the European eel *Anguilla anguilla* (L.). *J. Exp. Biol.* **205**, 2653-2663.

Liu, K., Nagase, H., Huang, C. G., Calamita, G. and Agre, P. (2006). Purification and functional characterization of aquaporin-8. *Biol. Cell* **98**, 153-161.

Ma, T., Yang, B. and Verkman, A. S. (1997). Cloning of a novel water and urea-permeable aquaporin from mouse expressed strongly in colon, placenta, liver, and heart. *Biochem. Biophys. Res. Commun.* **240**, 324-328.

Madsen, S. S., Olesen, J. H., Bedal, K., Engelund, M. B., Velasco-Santamaría, Y. M. and Tipsmark, C. K. (2011). Functional characterization of water transport and cellular localization of three aquaporin paralogs in the salmonid intestine. *Front. Physiol.* **2**, 56.

Martinez, A. S., Cutler, C. P., Wilson, G. D., Phillips, C., Hazon, N. and Cramb, G. (2005a). Regulation of expression of two aquaporin homologs in the intestine of the European eel: effects of seawater acclimation and cortisol treatment. *Am. J. Physiol.* **288**, R1733-R1743.

Martinez, A. S., Cutler, C. P., Wilson, G. D., Phillips, C., Hazon, N. and Cramb, G. (2005b). Cloning and expression of three aquaporin homologues from the European eel (*Anguilla anguilla*): effects of seawater acclimation and cortisol treatment on renal expression. *Biol. Cell* **97**, 615-627.

McDonald, M. D. (2007). The renal contribution to salt and water balance. In *Fish Osmoregulation* (ed. B. Baldisserotto, J. M. M. Romero and B. G. Kapoor), pp. 322-345. Enfield, NH: Science Publishers.
Moghadam, H. K., Ferguson, M. M. and Danzmann, R. G. (2011). Whole genome duplication: challenges and considerations associated with sequence orthology assignment in Salmoninae. *J. Fish Biol.* **79**, 561-574.
Notredame, C., Higgins, D. G. and Heringa, J. (2000). T-Coffee: a novel method for fast and accurate multiple sequence alignment. *J. Mol. Biol.* **302**, 205-217.
Olsvik, P. Å., Lie, K. K., Jordal, A. E., Nilsen, T. O. and Hordvik, I. (2005). Evaluation of potential reference genes in real-time RT-PCR studies of Atlantic salmon. *BMC Mol. Biol.* **6**, 21.
Pfaffl, M. W. (2001). A new mathematical model for relative quantification in real-time RT-PCR. *Nucleic Acids Res.* **29**, e45.
Raldúa, D., Otero, D., Fabra, M. and Cerdà, J. (2008). Differential localization and regulation of two aquaporin-1 homologs in the intestinal epithelia of the marine teleost *Sparus aurata*. *Am. J. Physiol.* **294**, R993-R1003.
Ronquist, F. and Huelsenbeck, J. P. (2003). MrBayes 3: Bayesian phylogenetic inference under mixed models. *Bioinformatics* **19**, 1572-1574.
Rozen, S. and Skaletsky, H. J. (2000). Primer3 on the WWW for general users and for biologist programmers. In *Bioinformatics Methods and Protocols: Methods in Molecular Biology* (ed. S. Krawetz, and S. Misener), pp. 365-386. Totowa, NJ: Humana Press.
Saparov, S. M., Liu, K., Agre, P. and Pohl, P. (2007). Fast and selective ammonia transport by aquaporin-8. *J. Biol. Chem.* **282**, 5296-5301.
Smith, H. W. (1932). The absorption and excretion of water and salts by marine teleosts. *Q. Rev. Biol.* **7**, 1-26.
Sundell, K. S. and Sundh, H. (2012). Intestinal fluid absorption in anadromous salmonids: importance of tight junctions and aquaporins. *Front. Physiol.* **3**,388.
Sundell, K., Jutfelt, F., Ágústsson, T., Olsen, R., Sandblom, E., Hansen, T. and Björnsson, B. T. (2003). Intestinal transport mechanisms and plasma cortisol levels during normal and out-of-season parr-smolt transformation of Atlantic salmon, *Salmo salar*. *Aquaculture* **222**, 265-285.
Suyama, M., Torrents, D. and Bork, P. (2006). PAL2NAL: robust conversion of protein sequence alignments into the corresponding codon alignments. *Nucleic Acids Res.* **34 Web Server issue**, W609-W612.
Swafford, D. L. (2002). *PAUP*. Phylogenetic Analysis Using Parsimony (*and Other Models)*. Version 4.0b10 for Macintosh. Sunderland, MA: Sinauer Associates.
Tingaud-Sequeira, A., Calusinska, M., Finn, R. N., Chauvigné, F., Lozano, J. and Cerdà, J. (2010). The zebrafish genome encodes the largest vertebrate repertoire of functional aquaporins with dual paralogy and substrate specificities similar to mammals. *BMC Evol. Biol.* **10**, 38.
Tipsmark, C. K., Kiilerich, P., Nilsen, T. O., Ebbesson, L. O. E., Stefansson, S. O. and Madsen, S. S. (2008). Branchial expression patterns of claudin isoforms in Atlantic salmon during seawater acclimation and smoltification. *Am. J. Physiol.* **294**, R1563-R1574.
Tipsmark, C. K., Sørensen, K. J. and Madsen, S. S. (2010). Aquaporin expression dynamics in osmoregulatory tissues of Atlantic salmon during smoltification and seawater acclimation. *J. Exp. Biol.* **213**, 368-379.
Tritto, S., Gastaldi, G., Zelenin, S., Grazioli, M., Orsenigo, M. N., Ventura, U., Laforenza, U. and Zelenina, M. (2007). Osmotic water permeability of rat intestinal brush border membrane vesicles: involvement of aquaporin-7 and aquaporin-8 and effect of metal ions. *Biochem. Cell Biol.* **85**, 675-684.
Usher, M. L., Talbot, C. and Eddy, F. B. (1988). Drinking in Atlantic salmon smolts transferred to seawater and the relationship between drinking and feeding. *Aquaculture* **73**, 237-246.
Wood, C. M. and Grosell, M. (2012). Independence of net water flux from paracellular permeability in the intestine of *Fundulus heteroclitus*, a euryhaline teleost. *J. Exp. Biol.* **215**, 508-517.
Yang, B., Zhao, D., Solenov, E. and Verkman, A. S. (2006). Evidence from knockout mice against physiologically significant aquaporin 8-facilitated ammonia transport. *Am. J. Physiol.* **291**, C417-C423.
Zapater, C., Chauvigné, F., Norberg, B., Finn, R. N. and Cerdà, J. (2011). Dual neofunctionalization of a rapidly evolving aquaporin-1 paralog resulted in constrained and relaxed traits controlling channel function during meiosis resumption in teleosts. *Mol. Biol. Evol.* **28**, 3151-3169.
Zapater, C., Chauvigné, F., Fernández-Gómez, B., Finn, R. N. and Cerdà, J. (2013). Alternative splicing of the nuclear progestin receptor in a perciform teleost generates novel mechanisms of dominant-negative transcriptional regulation. *Gen. Comp. Endocrinol.* **182**, 24-40.

Table S1. Accession numbers of sequences used in the study

Accession #	Ortholog	Animal	Species	Class/Rank	Order	Family
Aqp8aa						
ENSONIP00000024898	Aqp8aa	Nile tilapia	*Oreochromis niloticus*	Acanthomorpha	Perciformes	Cichlidae
ENSGACP00000012041	Aqp8aa	Three-spined stickleback	*Gasterosteus aculeatus*	Acanthomorpha	Gasterosteiformes	Gasterosteidae
ENSGMOP00000001261	Aqp8aa	Atlantic cod	*Gadus morhua*	Acanthomorpha	Gadiformes	Gadidae
CU071487	Aqp8aa	Rainbow trout	*Oncorhynchus mykiss*	Protacanthopterygii	Salmoniformes	Salmonidae
SsAqp8aa1	Aqp8aa1	Atlantic salmon	*Salmo salar*	Protacanthopterygii	Salmoniformes	Salmonidae
DW573347	Aqp8aa2	Atlantic salmon	*Salmo salar*	Protacanthopterygii	Salmoniformes	Salmonidae
EV367413	Aqp8aa	Lake whitefish	*Coregonus clupeaformis*	Protacanthopterygii	Salmoniformes	Salmonidae
ENSDARP00000066381	Aqp8aa	Zebrafish	*Danio rerio*	Ostariophysi	Cypriniformes	Cyprinidae
FJ655386	Aqp8aa	Zebrafish	*Danio rerio*	Ostariophysi	Cypriniformes	Cyprinidae
CK402738	Aqp8aa	Blue catfish	*Ictalurus furcatus*	Ostariophysi	Siluriformes	Ictaluridae
BAH89254	Aqp8aa	Japanese eel	*Anguilla japonica*	Elopomorpha	Anguilliformes	Anguillidae
Aqp8ab						
ENSONIP00000024897	Aqp8ab	Nile tilapia	*Oreochromis niloticus*	Acanthomorpha	Perciformes	Cichlidae
EB039337	Aqp8ab	Atlantic halibut	*Hippoglossus hippoglossus*	Acanthomorpha	Pleuronectiformes	Pleuronectidae
ACQ57933	Aqp8ab	Sablefish	*Anoplopoma fimbria*	Acanthomorpha	Scorpaeniformes	Anoplopomatidae
ENSGACP00000019141	Aqp8ab	Three-spined stickleback	*Gasterosteus aculeatus*	Acanthomorpha	Gasterosteiformes	Gasterosteidae
ENSORLP00000003812	Aqp8ab	Medaka	*Oryzias latipes*	Acanthomorpha	Beloniformes	Adrianichthyidae
ENSGMOP00000016961	Aqp8ab	Atlantic cod	*Gadus morhua*	Acanthomorpha	Gadiformes	Gadidae
CU071568	Aqp8ab	Rainbow trout	*Oncorhynchus mykiss*	Protacanthopterygii	Salmoniformes	Salmonidae
SsAqp8ab1	Aqp8ab	Atlantic salmon	*Salmo salar*	Protacanthopterygii	Salmoniformes	Salmonidae
ENSDARP00000096730	Aqp8ab	Zebrafish	*Danio rerio*	Ostariophysi	Cypriniformes	Cyprinidae
EU341834	Aqp8ab	Zebrafish	*Danio rerio*	Ostariophysi	Cypriniformes	Cyprinidae
DT136626	Aqp8ab	Fathead minnow	*Pimephales promelas*	Ostariophysi	Cypriniformes	Cyprinidae
DT342244	Aqp8ab	Fathead minnow	*Pimephales promelas*	Ostariophysi	Cypriniformes	Cyprinidae
ADO28238	Aqp8ab	Blue catfish	*Ictalurus furcatus*	Ostariophysi	Siluriformes	Ictaluridae
Aqp8b						
ENSTRUP00000007329	Aqp8b	Torafugu	*Takifugu rubripes*	Acanthomorpha	Tetraodontiformes	Tetraodontidae
BAL44700	Aqp8b	Mefugu	*Takifugu obscurus*	Acanthomorpha	Tetraodontiformes	Tetraodontidae
ENSTNIP00000021161	Aqp8b	Green-spotted pufferfish	*Tetraodon nigroviridis*	Acanthomorpha	Tetraodontiformes	Tetraodontidae
DQ889225	Aqp8b	Gilthead seabream	*Sparus aurata*	Acanthomorpha	Perciformes	Sparidae
GO620173	Aqp8b	Sablefish	*Anoplopoma fimbria*	Acanthomorpha	Scorpaeniformes	Anoplopomatidae
ENSGACP00000015550	Aqp8b	Three-spined stickleback	*Gasterosteus aculeatus*	Acanthomorpha	Gasterosteiformes	Gasterosteidae
GE808463	Aqp8b	Copper rockfish	*Sebastes caurinus*	Acanthomorpha	Scorpaeniformes	Sebastidae
EB038315	Aqp8b	Atlantic halibut	*Hippoglossus hippoglossus*	Acanthomorpha	Pleuronectiformes	Pleuronectidae
DV567193	Aqp8b	European flounder	*Platichthys flesus*	Acanthomorpha	Pleuronectiformes	Pleuronectidae
FE950965	Aqp8b	Turbot	*Scophthalmus maximus*	Acanthomorpha	Pleuronectiformes	Scophthalmidae
AFQ36924	Aqp8b	Sockeye salmon	*Oncorhynchus nerka*	Protacanthopterygii	Salmoniformes	Salmonidae
AFQ36926	Aqp8b	Chum salmon	*Oncorhynchus keta*	Protacanthopterygii	Salmoniformes	Salmonidae
SsAqp8b	Aqp8b	Atlantic salmon	*Salmo salar*	Protacanthopterygii	Salmoniformes	Salmonidae
ENSDARP00000005510	Aqp8b	Zebrafish	*Danio rerio*	Ostariophysi	Cypriniformes	Cyprinidae
FJ695516	Aqp8b	Zebrafish	*Danio rerio*	Ostariophysi	Cypriniformes	Cyprinidae